R2-B.3: Multi-Functional Nano-Electro-Opto-Mechanical Sensing Platform

I. PARTICIPANTS INVOLVED FROM JULY 1, 2019 TO JUNE 30, 2020

Faculty/Staff			
Name	**Title**	**Institution**	**Email**
Matteo Rinaldi	PI	NEU	rinaldi@ece.neu.edu
Zhenyun Qian	Research Faculty	NEU	qian@ece.neu.edu
Graduate, Undergraduate and REU Students			
Name	**Degree Pursued**	**Institution**	**Month/Year of Graduation**
Sungho Kang	PhD	NEU	05/2021
Vageeswar Rajaram	PhD	NEU	12/2020
Sila Calisgan	PhD	NEU	5/2022

II. PROJECT DESCRIPTION

A. Project Overview

Infrared-based human detection technologies have been extensively used in motion-triggered automation, indoor/outdoor security, search-and-rescue, and many other applications. The relatively high-power consumption of state-of-the-art motion detectors limits their battery life and increases the maintenance cost of sensor networks deployed in remote or hazardous locations. Passive infrared (PIR) is one of the key sensing technologies being utilized in such short-range persistent surveillance. Current PIR sensors have a limited lifetime when deployed in places like caves, tunnels, mines and underground facilities where energy harvesting (e.g., sunlight) is not available. However, persistent surveillance of such environments in proximity of the border is the most important means for border patrol to prevent smuggling or intrusion in restricted areas.

By exploiting our deep scientific knowledge of uncooled infrared (IR) detectors and zero-power microelectromechanical systems, we have developed wireless miniaturized human detectors with near-zero standby power (<10 nW) for applications in underground caves and tunnels. We developed an ultraminiaturized (coin-size), low-cost, and easily retrofitted wireless IR sensor capable of continuously monitoring the appearance of thermal radiation from the human body without consuming any power in standby (i.e., when human bodies are not present). The wireless IR sensor wakes up (i.e., drains power from the battery) only upon detection of the presence of humans nearby to transmit a radio frequency signal indicating the location of the human activity event. The miniaturized wireless IR sensors can be easily retrofitted to hide in the walls of underground caves and tunnels; and, thanks to the complete elimination of standby power consumption, it can wirelessly reveal thousands of intrusion events without draining the sensor coin battery (lifetime extended to approximately ten years, limited by battery self-discharge).

B. State of the Art and Technical Approach

The state-of-the-art motion detectors heavily rely on their limited power source (i.e., battery), leading to a short sensor lifetime, requiring high maintenance cost associated with the sensor network deployment in remote or hazardous locations. For example, solar-powered integrated fixed towers (IFT) equipped with radar, day and night cameras, and thermal imaging were deployed along the southwest border to provide long-range persistent surveillance enhance the situational awareness. Furthermore, the border patrol heavily relies on portable systems and unattended ground sensors (UGS) to address areas where rugged terrain and dense ground cover may allow adversaries to penetrate through blind spots or avoid the coverage areas of fixed surveillance systems. Passive infrared (PIR) sensors have been utilized in short-range persistent surveillance; nevertheless, their high dependence on external energy for sensor operation (such as sunlight) inhibits their deployment in places like caves, tunnels, mines, and underground facilities [1].

On the other hand, our technologies utilize the energy of infrared radiation emitted from a human body to operate and determine the presence of the person within a detection range without consuming any electrical power. We leveraged our deep scientific knowledge of uncooled infrared detectors and zero-power microsensing systems to develop wireless, miniaturized human detectors with near-zero standby power for applications in underground caves and tunnels. The proposed approach relies on both the spectrally selective thermal detectors technology developed under the ALERT project R2-B.3 [2, 3] and the zero-power infrared (ZIR) digitizing sensors technology developed under the DARPA N-ZERO program [4]. The core element of the technology is a micromechanical switch that is selectively triggered by IR radiation above a threshold (Figure 1). More specifically, the device selectively harvests energy contained in the specific IR signal of interest (i.e., IR radiation from human bodies) and uses it to mechanically create a conducting channel between two electrical contacts (i.e., a large, sharp off-to-on state transition with an on/off conductance ratio >10^{12} and a practically infinite subthreshold slope) when the strength of the signal is above a predetermined threshold, without the need of any additional power source. Differently from PIR technology, our sensors produce a binary signal directly corresponding to the presence and absence of the triggering IR radiation and do not require any active electronics for signal conditioning.

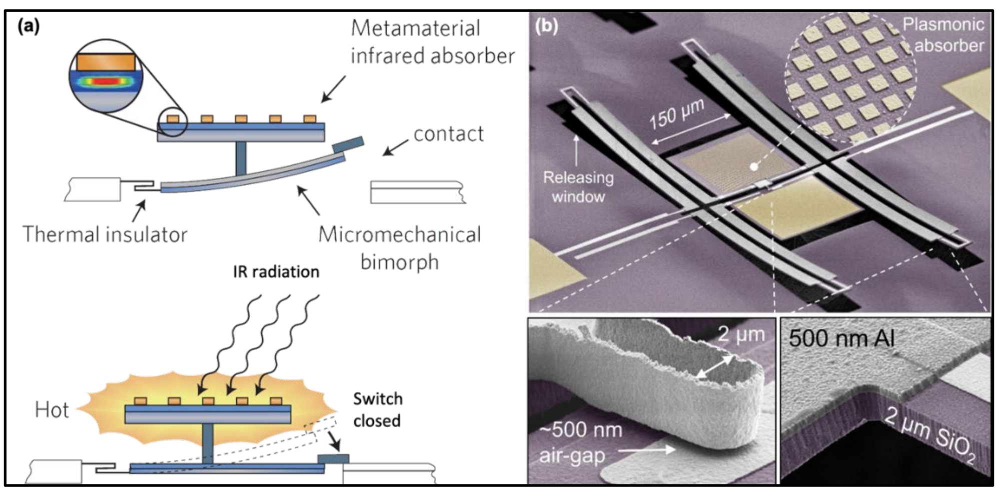

Figure 1: (a) Working principle of zero-power IR sensors [5]; (b) scanning electron microscope image of a fabricated device [4].

Caves and tunnels have much less temperature variability than surface domains that are directly exposed to solar flux, precipitation, and air convection. Moreover, rocks and concretes have 20% to 30% lower emissivity than skin and cloth (Figure 2a) at the IR wavelengths a human body emits. A relatively constant and large contrast between human bodies and the background guarantees a reliable threshold-based detection. The main research challenges preventing the implementation of such micromechanical photoswitch (MP) based zero-power human detectors are (1) the integration of ultrathin IR absorbers that feature near-unity absorption in a broad mid- to long-IR spectral band (6–12 μm) and (2) the further scaling of the MP detection threshold to tens of nW to enable long range detection of human body radiation.

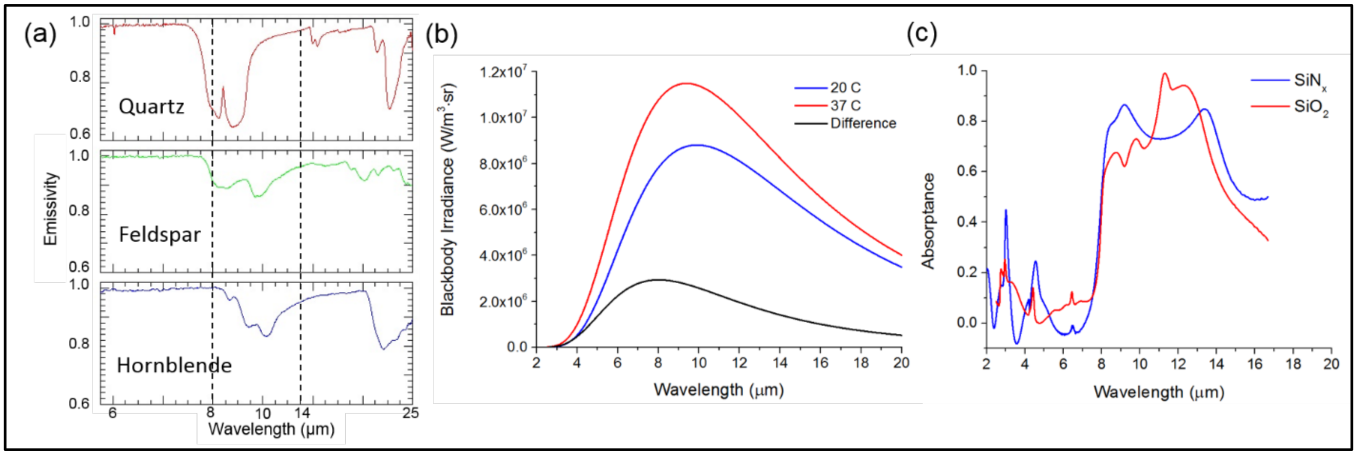

Figure 2: (a) Emissivity spectra of three common constituents of rocks. The emissivity of skin and cloth are between 0.95 and 1. (b) Radiative emission spectra of blackbody sources at 37°C and 20°C, and the difference between the two spectra. (c) Measured absorption spectra of 2-μm SiN_x and SiO_2 [6].

Human bodies emit IR radiation mainly at 8–14 μm. In order to discriminate the background radiation, the sensor should be configured to capture the difference between the two emission spectra (Figure 2b), which peaks at ~8 μm with a wide spread from 6–12 μm. To effectively collect most of the IR energy, we demonstrated broadband long-wavelength IR absorbers composed of a 2-μm SiO_2 slab backed by a metal reflector. A ZIR sensor with an ultralow IR detection threshold of ~140 nW, suitable for human body detection, has been experimentally demonstrated by the PIs' team [7]. When detecting a human body from a distance, the available IR power will inevitably be smaller. Therefore, we further optimized the device design in terms of thermal isolation and IR absorption to scale down the detection threshold to ~40 nW, which corresponds to a detection range as far as 10 m with a focusing lens by adding a highly absorptive dielectric layer such as SiN_x or SiO_2 (Figure 2c). Another important aspect of the ZIR sensor is the reliability. The demonstrated prototypes have already been proven to have relatively high reliability for the envisioned application: over eight thousand consecutive on/off cycles without failure have been demonstrated [4]. Detectors based on single devices with a wide field of view or multiplexed microswitches with a concentrating lens that image different target areas are feasible with our technology. These passive, unpowered human detectors can trigger wireless alarm signals, which can start an action, such as turning on recording media that sits unpowered until the microswitch is closed, enabling unattended operation limited only by the open-circuit life of the accompanying battery.

C. Major Contributions

C.1. Device Design

An analytical model has been developed to improve the thermo-mechanical performance of the previously demonstrated zero-power IR photoswitches and previously verified with the commercially available computer-aided finite element model (FEM) simulation tool, COMSOL. The analytical model eliminates the need of numerical calculation, which can be time inefficient since each data point for each geometry combination involves more than nine parameters. On the other hand, the analytical model can be utilized to study the relationship between each variable geometric parameter and the sensor figure of merits (e.g., device threshold power, thermal sensitivity, stiffness, and time constant). The analytical program connects all the design parameters to find an optimized solution for each one and to analyze its trade-offs among different figures of merit. The new analytical approach considers the contribution of strain energy in each section of mechanical beams (i.e., two bimaterial beams and a thermal isolation region) via the fundamental solid mechanical modeling. On the other hand, the bimorph thermal actuator model was utilized to accurately describe IR-thermal properties of the sensor. The total device emissivity has been calculated based on the weighted emissivity of aluminum and silicon dioxide to take into consideration their difference in volume and, as a consequence, their different thermal mass. Most importantly, the thickness of the thermal isolation link is separated from the rest of cantilever (i.e., bimaterial beams and the IR absorbing/reflecting heads) in order to give an extra degree of freedom during the optimization process.

The analytical model was utilized to design a low IR threshold device to meet the required device sensitivity for the target application via the loop-based optimization process (Figure 3). The aim was to maintain the stiffness (k) similar to the one previously demonstrated (k = 0.02 N/m) while increasing the thermal sensitivity (S) as much as possible (it has been doubled from a value of 0.982 m/W to 2.10 m/W). Table 1 shows the figure of merits of the new design. Figure 4 helps understand the nine parameters we have been working on. L3, W3, and t3 refer to the length, width, and thickness of bimaterial legs, respectively; while L1, W1, t, L2, and W2 refer to the lengths, widths, and thickness of the isolation region link that connects the two bimaterial legs.

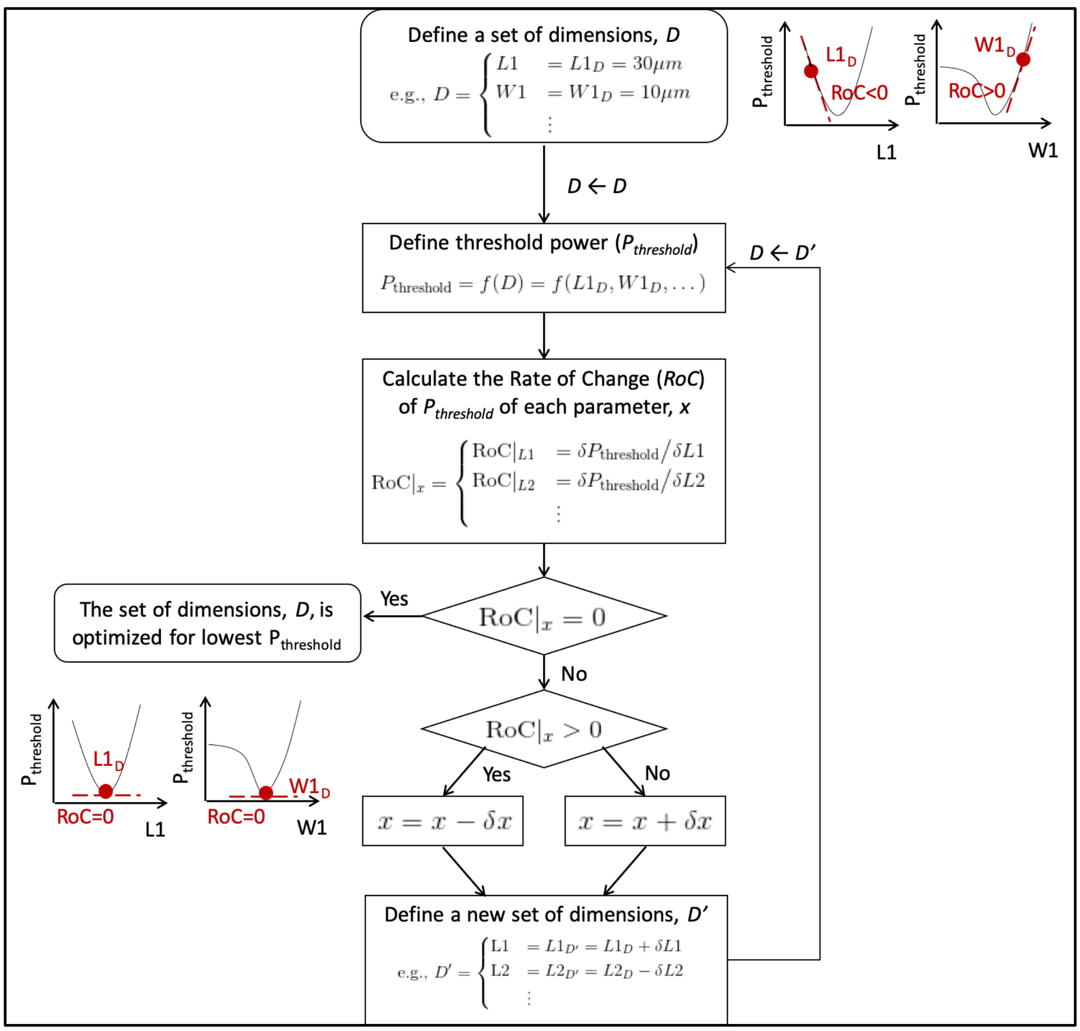

Figure 3: The loop-based optimization process for the low IR threshold device design.

Analytical Model	Previous Demonstration	Primary Design of the New Generation
Stiffness (N/m)	0.022	0.020
Thermal sensitivity (m/W)	0.982	2.100
Time constant (sec)	0.246	0.125
Threshold, 500 nm gap (nW)	509	240

Table 1: Primary design figures of merit.

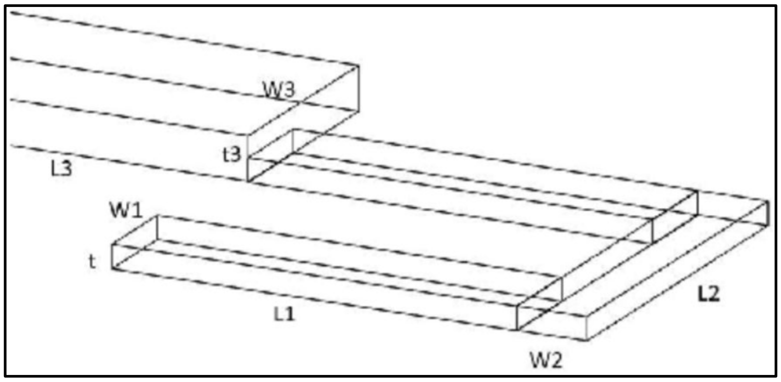

Figure 4: Graphical explanation on the parameters of Table 1 where *t3* = *t_ox* + *t_al*.

The stiffness and thermal sensitivity calculation based on the analytical model have been confirmed by Comsol simulations (Figure 5). The simulated stiffness of the device is 0.02 N/m, which agrees well with the analytical model (0.019 N/m). Furthermore, by applying 500 nW of incident IR power on the whole area of the head, we get a displacement of 1,060 nm, confirming also the analytical value of the thermal sensitivity to be 2.1 m/W.

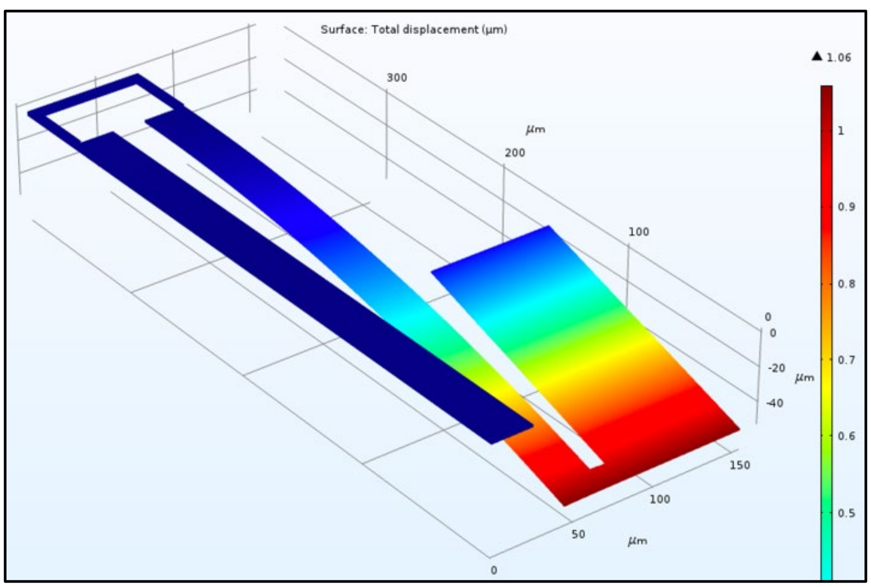

Figure 5: Comsol simulation of the primary design: displacement of 1,050 nm due to 500 nW applied on the head of the device.

The new mask layout includes the optimized device designs as primary devices with two types of contact tips: rectangular and triangular. Nonprimary (secondary) devices include other designs focused on the improvement of the thermal sensitivity with varying stiffnesses, as well as the designs focused on improving the time constant. Last but not least, proven designs from previous demonstrations, as well as some special designs (i.e., not fully supported by theory but with the potential of great advantages in certain aspects), were included in the mask layout. FEM Comsol simulations were employed to verify the effectiveness of most designs. The following shows which designs are included in the mask:

- Primary designs
    - Low threshold power
    - Rectangular and triangular contact tips
    - Different head sizes
- Secondary designs
    - Low time constant
    - High thermal sensitivity
- Other designs
    - Experimental designs
    - Array of primary designs
    - Test structures

C.2. Broadband Absorber Designs

The presence of a human can be detected using the thermal energy emitted in a long-wave infrared (LWIR) regime (e.g., a human body at 37°C has peak IR emissions at around λ = 8–12 μm). In order to harvest the LWIR electromagnetic energy efficiently, we designed different absorber designs that can be integrated in the existing IR sensor. We have demonstrated a LWIR photoswitch using the bulk dielectric (SiO_2) slab backed by an optically thick metal layer as the integrated absorber (Figure 6). The measured absorptance of such a bulk absorber shows consistently high absorptance in the spectral region of interest (η >60% in 8–16 μm). However, the device suffers asymmetry induced by the different material stacks in the absorbing and reflecting heads (a reflecting head has an additional optically thick metal layer as a reflector) (Figure 6). In order to minimize the device asymmetry, we have proposed the two possible absorber designs: (a) plasmonic-dielectric absorber; and (b) metal-germanium-metal absorber.

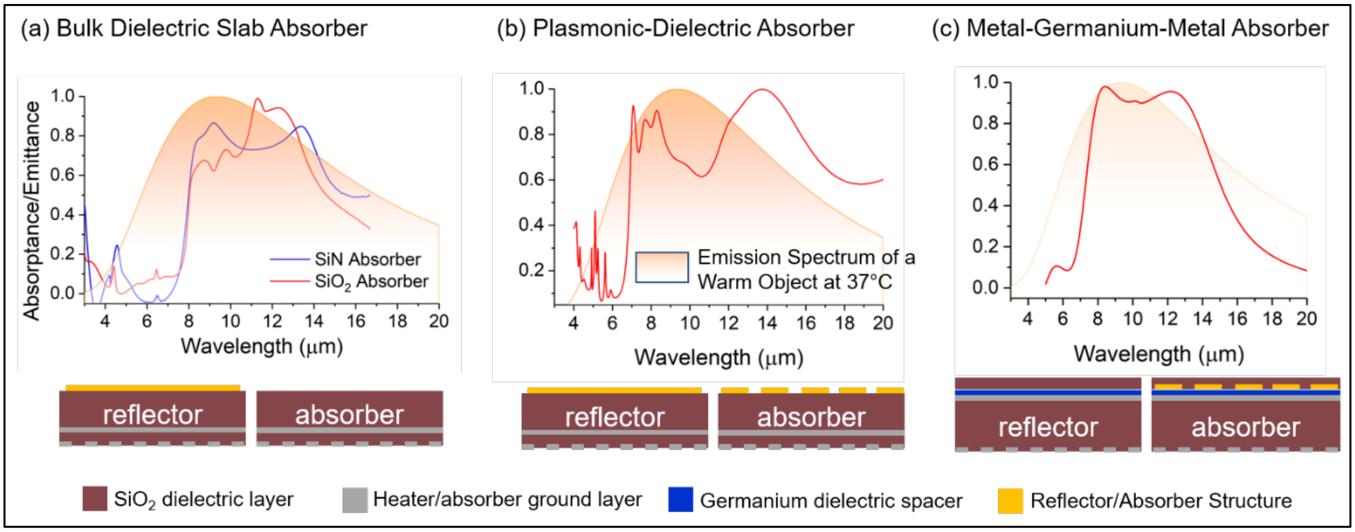

Figure 6: Proposed LWIR broadband absorbers for leaf temperature sensing.

The plasmonic-dielectric absorbers take advantage of both the high loss of SiO_2 slab due to the vibrational modes of longitudinal-optical phonons and the highly capacitive metamaterial sheet patterned on top of the dielectric slab. The numerical calculation (simulated with a commercially available full-wave simulation software, Computer Simulation Technology) shows a high absorptance in the LWIR regime with a broader absorption bandwidth (η >60% in λ = 7–20 μm) than the dielectric slab alone (Figure 6b). The metal-germanium-metal absorber shares the same working principles as the MIM IR absorbers demonstrated for spectrally selective near-IR and mid-wavelength IR absorption. This configuration replaces the SiO_2 subwavelength dielectric layer with an optically dense material, germanium, and the gold plasmonic nanostructures with high-loss metal layer, titanium, to achieve highly absorptive and broadband absorption in LWIR spectral regime. The numerical simulation shows a near-perfect absorption in the LWIR region of interest (η>90% in λ = 8–13 μm) (Figure 6c). Note that it will be necessary to incorporate a protective layer (such as an optically thin SiO_2 layer as shown in the cross-sectional schematic figure) to prevent from etching in an XeF_2 device release fabrication step. It is also worth noting that the proposed absorbers are designed such that they incorporate the microheaters in both absorbing and reflecting heads.

C.3. Fabrication and Characterization of New Devices

The photomasks of the new mask layout for the optimized devices were manufactured. Differently from the previous fabrication process, the new process involves three additional photomasks (eleven in total). The device design optimizations proposed previously were implemented in the new batch of devices. These recently fabricated devices were tested to verify whether the design changes had an effect on improving the device sensitivity. The sensitivity S is defined as the displacement induced at the tip of the switch contact per unit input power. For a given contact gap g, a larger S results in a smaller threshold P_t. One of the major design features of the new batch is the integration of microheaters on all devices to simulate the temperature rise caused by IR absorption. The integration of the heaters also affords an accurate and efficient way to quickly estimate the threshold and sensitivity of each device on the wafer. In the experiments described below, the sensitivity of the optimized device was calculated by measuring the threshold power and the contact gap.

To find the sensitivity, the voltage V_{heater} across the microheater (R = 63.8 kΩ) was increased until the power dissipated as heat was sufficiently high to actuate the contacts and close the switch. The value of this power is calculated by the equation $P_t = V_{heater}^2/R$. Note: the device was tested in a vacuum probe station to ensure that there was no heat loss through convection in air.

The status of the switch was monitored continuously by applying a separate bias V_{bias} across the switch terminals and monitoring the current using a source meter (Keithley 2450). Figure 7a shows the circuit schematic overlaid on an optical image of the tested device. The heater layer is on the bottom of the device while the electrical routing for the switch is on the top and is electrically insulated from the heater. Figure 7b shows the measured current across the switch as the heater is turned on and off with a V_{heater} that corresponds to a power just above P_{heater}. As shown, when triggered on, the current changes with a conductance ratio of more than 4 orders of magnitude from ~0.1 nA to 0.7 µA for a V_{bias} = 10 mV (the non-zero off current is due to instrument noise). This essentially demonstrates the zero subthreshold leakage of the switches, which is a key factor for zero standby power consumption. P_t for the tested device was measured to be 492 nW.

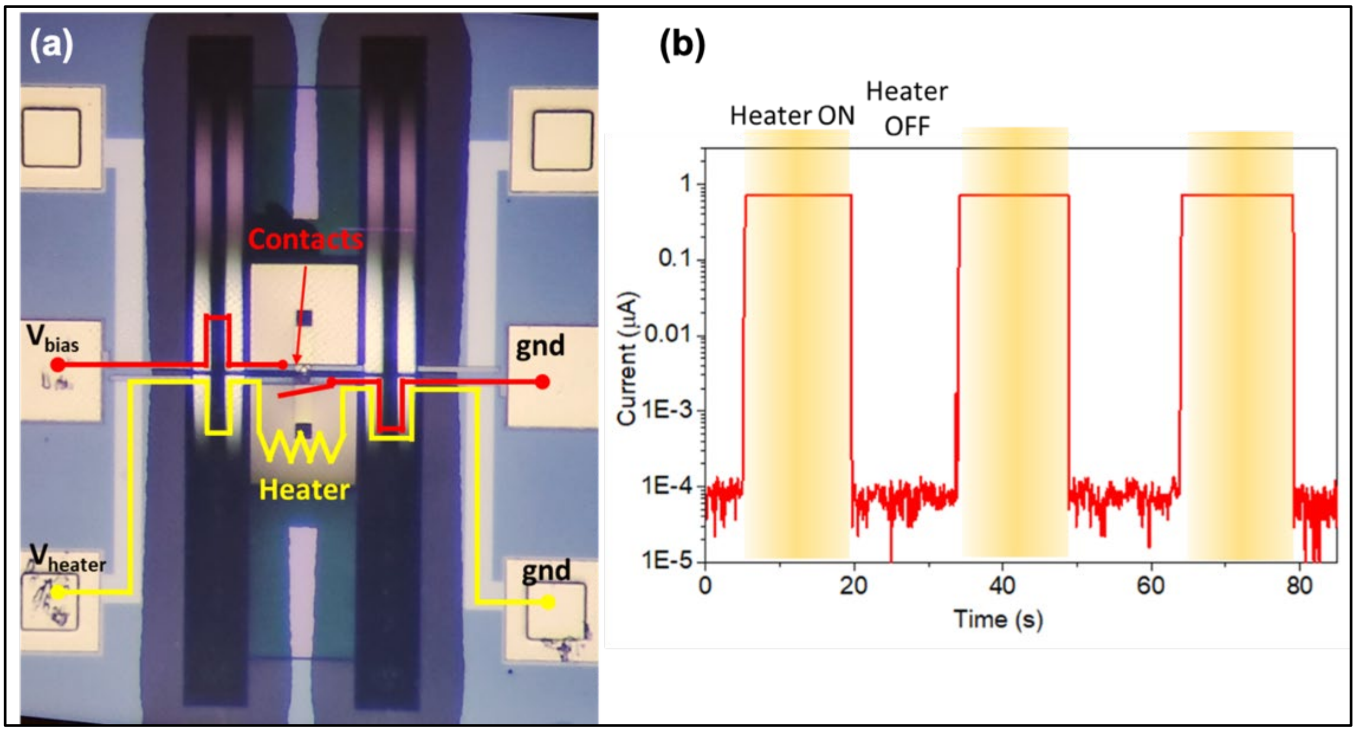

Figure 7: (a) Optical image of tested device with an overlay of the electrical routing schematic. (b) Current across the switch as the heater is turned on and off with a $P_{heater} \geq P_t$.

Next, the contact gap (g) was estimated using the pull-in voltage technique. Since the contacts are effectively a pair of capacitors with an overlap area A and a vacuum as a dielectric, increasing V_{bias} causes charges to accumulate on either contact. Since the contacts are attached to cantilevers (i.e., springs) the electrostatic force developed between the contacts due to these charges causes the contacts to move toward each other. At a certain Voltage $V_{bias} = V_{\text{pull-in}}$, the system becomes unstable and the contacts snap closed (i.e., pull-in). The value of this pull-in voltage is given by:

$$V_{pull\text{-}in} = \sqrt{\frac{8kg^3}{27\varepsilon_o A}}$$

where k is the effective stiffness of the cantilevers (0.0075 N/m from simulations). By sweeping the voltage V_{bias} (without applying any heater power) until the contacts close, $V_{pull\text{-}in}$ can be measured and g can be readily calculated. The overlap area A (67.7 µm^2) was measured using an optical microscope at high magnification. For the tested device, $V_{pull\text{-}in}$ = 2.23 V and thus g = 1.095 µm. This results in a sensitivity of the device $S = g/P_t$ = 2.22 nm/nW. This is very close to the designed sensitivity of 2.46 nm/nW (determined using analytical modeling). It is worth noting that this is an improvement of ~2.2 times over the previous designs. This experiment thus proves that the new designs indeed have a better sensitivity and thus can be used to achieve unprecedented threshold levels.

C.4. Zero-Power Human Detection

We successfully demonstrated zero-power detection of a hand (at a 16-inch distance) without using a focal lens, owing to the optimized micromechanical structure and thermal expansion material, hence the reduced threshold (Figure 8). We have characterized the infrared radiation from a human body at a varying angle (top, side, and front-facing) and distance (from 0.5 to 2.0 m), using a commercial thermal detector with an active area of 10-mm diameter (Figure 9). Furthermore, we have identified that using a Fresnel focusing lens, the available IR power density can be increased by more than 10 times, which drastically increases the working distance of our sensor. Because of the aforementioned results in terms of device optimization, characterization, and optics-level sensitivity improvement, we have successfully demonstrated a zero-power detection of a human body at ~13 feet distance (Figure 10).

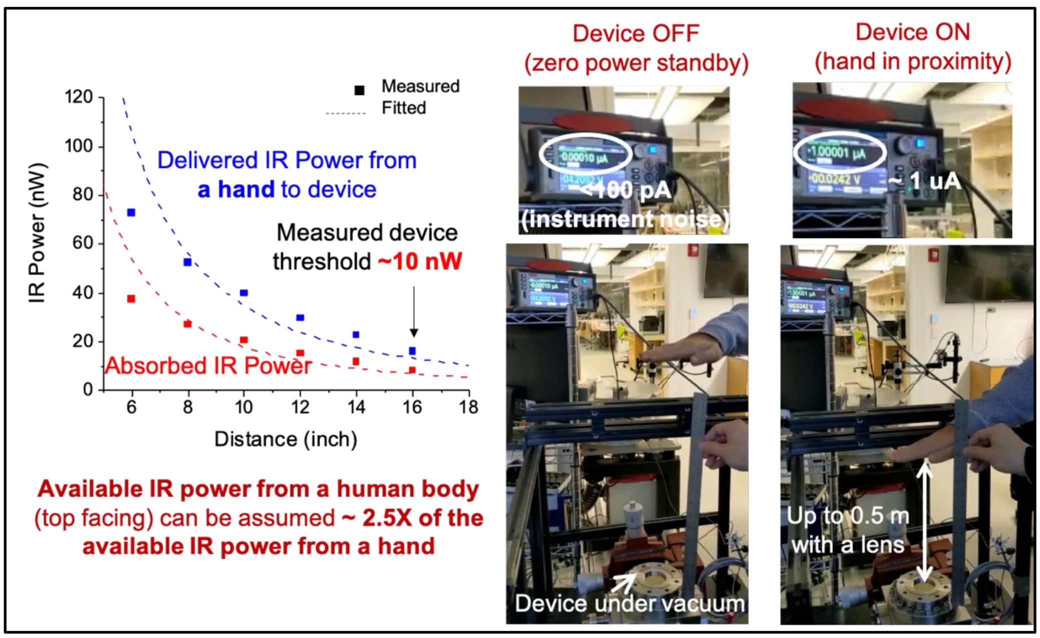

Figure 8: First demonstration of zero-power hand detection.

Tool:
Commercial thermal detector with active area of Φ 10 mm
(3489x larger than our sensor)

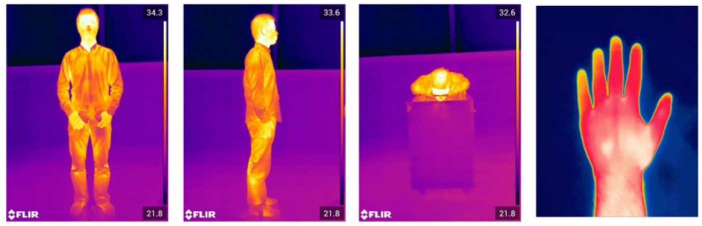

Measurement	Front Facing	Side Facing	Top Facing	Hand
Power @ 0.5m (1.6 ft)	~ 440 μW	~ 330 μW	~ 203 μW	~ 75 μW
Power @ 1m (3.3 ft)	~ 220 μW	~ 158 μW	~ 50 μW	~ 20 μW
Power @ 2m (6.6 ft)	~ 65 μW	~ 45 μW	~ 22 μW	~ 5 μW
Power density @ 1m	2.8 W/m^2	2.0 W/m^2	0.64 W/m^2	0.25 W/m^2
Power delivered to 150x150 μm^2 device @ 1m	63 nW	45 nW	14 nW	5.6 nW
Normalization	100%	~72%	~23%	~ 9%

Figure 9: Characterization of available IR power radiated from a human body at a varying angle and distance.

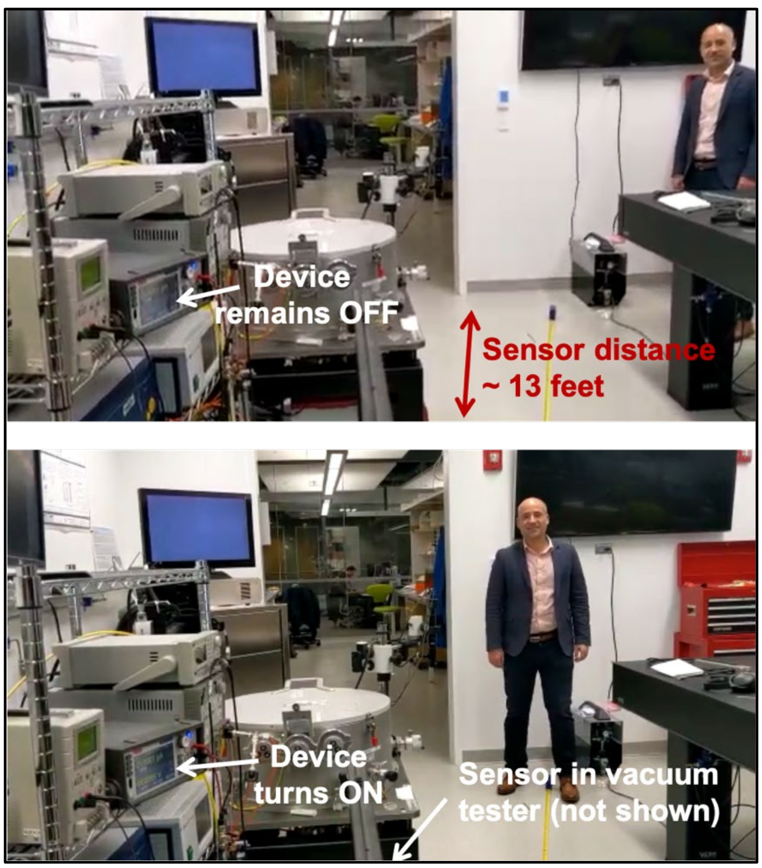

Figure 10: First demonstration of zero-power human detection.

D. *Milestones*

- **Design of optimized IR sensor with threshold ~40 nW (completed):** When detecting a human body from a larger distance, the delivered IR power to the sensor will inevitably be much smaller due to the inverse-square law. We successfully demonstrated a group of optimized sensor designs with a threshold as low as ~39.4 nW, which was verified through both the analytical model and finite element simulation.
- **Design of experimental setup for human body detection (completed):** The current experimental setup only supports incident infrared light from the top of the testing chamber. Measurement using only a hand instead of a full body as the target was performed for now. Modification of the existing setup with an additional optical path has been designed and implemented to support the test with a human body in horizontal direction (with varying distance) as the target.
- **Device fabrication and characterization (completed):** The first batch of newly designed sensors has been fabricated. The integrated heaters were utilized to measure the IR threshold. The ultra-low IR threshold reaching ~7 nW was demonstrated with a voltage bias. Full characterization was completed, and modified plans are being implemented for the next batch fabrication based upon the characterization. This includes the in situ test functionality for flipped heads, use of a high substrate resistance wafer, and sidewall coating to prevent unwanted pull-in.
- **Reliability test and design optimization (in progress):** The previously demonstrated prototypes have already been proven to have relatively high reliability for the envisioned application: over eight thousand consecutive on/off cycles without failure have been demonstrated. The proposed characterization of the common failure mechanism and demonstration of one million cycles of operation has been postponed after ~60% toward completion due to the ongoing laboratory shutdown due to COVID-19 restrictions.
- **Demonstration of a working prototype in lab environment (completed):** With design iteration, we experimentally demonstrated a working prototype of the zero-power infrared sensor capable of detecting a human body from more than ~4 meters away (expected to have >10-meter detection range, currently limited by the compartmented laboratory space).
- **Finalize a collaboration plan with United Technologies Corporation (completed):** The team has received a $550K grant from the National Science Foundation for a collaboration with United Technologies Corporation.

E. *Final Results at Project Completion (Year 7)*

We have successfully designed, fabricated, and characterized the first prototype of zero-power human detector suitable for realization of sensor networks deployed in remote or hazardous locations. This sensor network can be deployed with substantially low maintenance cost associated with sensor installation and management. We envision that the demonstrated work can significantly enhance border protection to prevent smuggling or intrusion in restricted areas where the conventional fixed surveillance system is not suitable. The following research works were conceived and successfully executed: (1) We have developed a rigorous thermomechanical analytical model to predict sensor performance to optimize the device geometries. The resulting device has shown much improved sensor performances (thermal sensitivity, stiffness, and device response time) compared to the previous generation, suitable for ultralow threshold IR radiation detection of a human body; (2) the new batch of devices was fabricated and characterized with the proper experimental setup, showing an ultralow IR detection threshold reaching ~7 nW; (3) we have successfully demonstrated the first zero-power human detection capability using the fabricated device with a working distance reaching ~4 meters; and (4) the team has secured two technology transition funding to develop minimum viable products for border protection and fire prevention applications.

III. RELEVANCE AND TRANSITION

A. Relevance of Research to the DHS Enterprise

- **Relevance #1/metrics:** IR digitizing microsystems that can remain dormant, with near-zero power consumption, until awakened by specific IR spectral signatures associated with a threat (e.g., human intrusion). These completely passive digitizing IR sensor microsystems can harvest the energy contained in a specific IR spectral signature (i.e., IR emission peaks of energetic materials) to produce a digitized output bit capable of waking up short-duty cycle powered electronics for further signal analysis and communications.
- **Relevance #2/metrics:** A wireless sensor network to be deployed in the difficult-to-reach places such as caves, tunnels, mines, and underground facilities. These ultraminiaturized (coin-size), low-cost, and easily retrofitted wireless IR sensor is capable of continuously monitoring the appearance of thermal radiation from human body, without consuming any power in standby.

B. Status of Transition at Project End

- The patent for the base technology was granted in May 2020.
- A provisional patent application was filed to protect the specific device designs developed in this work.
- An internal technology transition funding (GapFund360 Phase 1&2) was secured to develop the minimum viable product for occupancy sensing.
- External funding from the NSF technology translation program, Partnerships for Innovation, was secured to develop the minimum viable product for flame detection based on the same core technology developed in this project.
- A startup company, Zepsor Technologies, has been founded aiming to bring to market zero standby power sensors for various internet-of-things applications including distributed wireless fire monitoring systems, battery-less infrared sensor tags for occupancy sensing, and distributed wireless monitoring systems of plant health parameters for digital agriculture.

C. Transition Pathway and Future Opportunities

- Awarded with internal funding for technology transfer (GapFund360), the project targets the development of battery-less IR sensor tags for reliable occupancy sensing in indoor environment, which is suitable for many DHS-related (DHS: Department of Homeland Security) applications such as airport security.
- Potential commercialization partners (Pendar Technologies, Analog Devices, and Boeing) have already been engaged with performance testing and transition development work.
- The PI holds intellectual property of the technology relevant to the project.
- Prototypes of the technology are being fabricated at Northeastern University for use and testing.

- The proof of concept will be shared with the identified potential customers to explore technology transition: DHS, Defense Advanced Research Projects Agency (DARPA), Analog Devices, Qualcomm, Pendar Technologies, Boeing, and Avago.

D. Customer Connections

- DHS
- United Technologies Corporation: Joseph Mantese
- DARPA Microsystems Technology Office: Ronald Polcawich, Benjamin Griffin, and Whitney Mason
- Air Force Office of Science Research: Kenneth Goretta, Gernot Pomrenke, and Harold Weinstok
- Analog Devices
- Qualcomm
- RF Micro Devices
- Pendar Technologies
- Avago

IV. PROJECT ACCOMPLISHMENTS AND DOCUMENTATION

A. Education and Workforce Development Activities

1. Course, Seminar, and/or Workshop Development
    a. 2019 fall semester course: Introduction to MEMS
2. Student Internship, Job, and/or Research Opportunities
    a. Research assistantship for two graduate students

B. Peer Reviewed Journal Articles

1. Qian, Z., Rajaram, V., Kang, S., & Rinaldi, M. "High Figure-of-Merit NEMS Thermal Detectors Based on 50-nm Thick AlN Nano-Plate Resonators." *Applied Physics Letters, 115*(26), 2019. https://doi.org/10.1063/1.5128643.

C. Poster Sessions

1. "Zero-Power Wireless Sensor Nodes for Unattended Threat Monitoring." Presented by Ryan Kang and Vageeswar Rajaram. 7th ALERT Industrial Advisory Board Meeting Poster Session. Northeastern Innovation Campus, Burlington, MA. 4 November 2019.

D. Other Presentations

1. "Research Highlight: Zero-Power Sensors." Presented by Matteo Rinaldi. 7th ALERT Industrial Advisory Board Meeting. Northeastern Innovation Campus, Burlington, MA. 4 November 2019.

E. *Technology Transfer/Patents*

1. Patent Awarded
    a. Zero Power Plasmonic Microelectromechanical Devices. Patent Number US 10,643,810 B2. Granted May 2020.

F. *Patent Applications Filed (Including Provisional Patents)*

1. Zero Power Micromechanical Switch-Based Sensing and Monitoring System, PCT Application No. PCT PCT/US2020/014478.
2. Zero-Power Wireless System for Crop Water Content Monitoring, PCT Application No. PCT/US2020/014427.

V. REFERENCES

[1] Homeland Security, "Integrated Fixed Towers."

[2] S. D. Calisgan et al., "Spectroscopic Chemical Sensing Based on Narrowband MEMS Resonant Infrared Detectors," in *2018 IEEE SENSORS*, 2018, vol. 0, pp. 1–4.

[3] S. Kang, Z. Qian, V. Rajaram, S. D. Calisgan, and M. Rinaldi, "Chip-Scale MEMS-CMOS Multispectral Infrared Chemical Sensor," *2019 IEEE Micro Electro Mech. Syst.*, no. January, pp. 133–136, 2019.

[4] Z. Qian, S. Kang, V. Rajaram, C. Cassella, N. E. McGruer, and M. Rinaldi, "Zero-Power Infrared Digitizers Based on Plasmonically Enhanced Micromechanical Photoswitches," *Nat. Nanotechnol.*, vol. 12, no. 10, pp. 969–973, Sep. 2017.

[5] V. A. Aksyuk, "Internet of Things: Sensing without Power," *Nat. Nanotechnol.*, vol. 12, no. 10, pp. 940–941, Sep. 2017.

[6] J. Kischkat et al., "Mid-Infrared Optical Properties of Thin Films of Aluminum Oxide, Titanium Dioxide, Silicon Dioxide, Aluminum Nitride, and Silicon Nitride," *Appl. Opt.*, vol. 51, no. 28, p. 6789, 2012.

[7] S. Kang, S. Calisgan, Z. Qian, V. Rajaram, N. McGruer, and M. Rinaldi, "Broadband Long-Wavelength Infrared Micromechanical Photoswitch for Zero-Power Human Detection," in *2018 Solid-State, Actuators, and Microsystems Workshop Technical Digest*, 2018, no. d, pp. 187–189.